Miniaturized microstrip diplexer with broadband characteristics using metamaterials

I. A. MOCANU, T. PETRESCU[a]
[a]*Microwave Department, University Politehnica of Bucharest, Bucharest, Romania*

In this paper, there is presented a metamaterial diplexer designed and implemented in microstrip technology. It uses two types of structures which allow to minimize the dimensions of the overall device and to enhance the working bandwidth. An equivalent model of the structure and analytical expressions are given as a starting point in the optimization process. The measurements confirm the theoretical and simulated results. The transfer characteristic for the first channel is from 2GHz to 4.25GHz, respectively for the second channel is from 4.25GHz to 7GHz.

(Received June 10, 2015; accepted September 29, 2016)

Keywords: Metamaterials, Microstrip diplexer, Strong coupling, Bradband device

1. Introduction

The need for devices with improved performances and smaller dimensions can be nowadays achieved by using new types of materials. The class of metamaterials shows interesting and versatile properties not available in nature. The mostly used are the Left Handed (LH) structures obtained artificially by chaining certain number of unit cells. Each unit cell must satisfy the homogenous condition, which can be postulated for microwave domain as: the length of the unit cell must be much smaller than a quarter of the wavelength corresponding to the working frequency [1]. As long as this condition is fulfilled we can use the term of material for this new types of artificial structures.

The cells can be implemented using different technologies such as: microstrip, coplanar, stripline, each technology exhibiting advantages and disadvantages [2], [3], [4]. In this paper we start our study from a microstrip implementation of a metamaterial which is designed to work at a central frequency of 4.5GHz.

In order to better understand the propagation phenomenon which appears on these microwave structures, the most common approach is the transmission line one. It implies using a lumped element equivalent model for the microstrip unit cells [1]. The main disadvantage of this method is that it gives an approximate behavior of the unit cell because lumped elements are influenced by the frequency changes. Still, it can be used as a starting point in the design of the microstrip metamaterial.

We consider in this paper the Composite Right Left Handed (CRLH) structures which exhibit both conventional behavior (Right Handed-RH one) and unconventional behavior (Left Handed-LH one) [5]. The Left Handed behavior allows us to use two coupled metamaterial structures in order to achieve a very tight coupling, up to 0dB and to create a diplexer with enhanced working bandwidth and miniaturized dimensions [6].

2. Experimental

In order to implement the metamaterial main structure in microstrip technology, we start by designing a unit cell. The Left Handed properties can be achieved by using a structure made of an interdigital capacitor and a shunt stub inductor as shown in Fig. 1 [1].

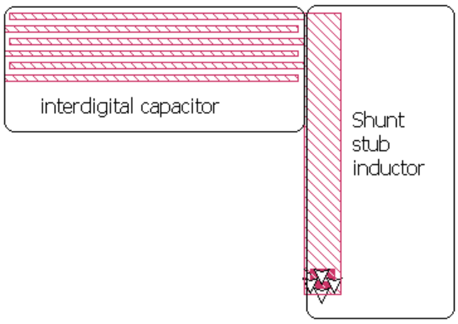

Fig. 1. Microstrip metamaterial unit cell

Both the interdigital capacitor and the shunt stub inductor present parasitic effects which give the Right Handed behavior of the structure. These effects are considered by the simplified equivalent model in Fig. 2 [1].

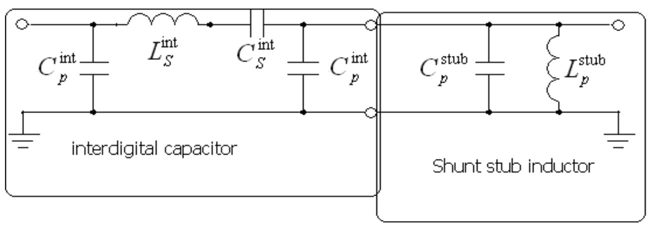

Fig. 2. Simplified equivalent model for the microstrip metamaterial unit cell

The analytical expression for L_S^{int} in Fig. 2 is given by [7]:

$$L_S^{\text{int}}[H]=\frac{\mu_0 l}{4\pi}\left[2\operatorname{arsinh}\left(\frac{l}{w_{tot}}\right)+2\frac{l}{w_{tot}}\operatorname{arsinh}\left(\frac{w_{tot}}{l}\right)-\frac{2}{3}\frac{\left(w_{tot}{}^2+l^2\right)^{3/2}}{lw_{tot}{}^2}+\frac{2}{3}\left(\frac{l}{w_{tot}}\right)^2+\frac{2}{3}\frac{w_{tot}}{l}\right] \quad (1)$$

where: $\mu_0=4\pi\cdot10^{-7}\,\text{H/m}$, l is the length of the interdigital capacitor and w_{tot} is the width of the whole digits of the interdigital capacitor.

The C_S^{int} value can be computed using the formula [8]:

$$C_S^{\text{int}}(pF)=\frac{\varepsilon_r\cdot10^{-3}}{18\pi}\cdot\frac{K(k)}{K'(k)}\cdot(n-1)\cdot\frac{l}{10^{-6}} \quad (2)$$

where: ε_r is the relative permittivity of the substrate, n is the number of digits, l is the length of the interdigital capacitor and $K(k)$ and $K'(k)$ are elliptic integral, respectively its derivate approximated by the following relations:

$$K(k)=\int_0^{\pi/2}\left(1-k\sin^2 t\right)^{-0,5}dt\cong\frac{\pi}{2}+\frac{\pi}{8}\frac{k^2}{1-k^2}-\frac{\pi}{16}\frac{k^4}{1-k^2} \quad (3)$$

$$K'(\sqrt{1-k^2})=\int_0^{\pi/2}\left(1-\sqrt{1-k^2}\sin^2 t\right)^{-0,5}dt \quad (4)$$

$$K'(\sqrt{1-k^2})\cong\frac{\pi}{2}+\frac{\pi}{8}\frac{\left(\sqrt{1-k^2}\right)^2}{1-\left(\sqrt{1-k^2}\right)^2}-\frac{\pi}{16}\frac{\left(\sqrt{1-k^2}\right)^4}{1-\left(\sqrt{1-k^2}\right)^2} \quad (5)$$

with:

$$k=\tan^2\left(\frac{a\pi}{4b}\right), \quad (6)$$

$$a=\frac{w}{2}, b=\frac{w+s}{2}. \quad (7)$$

and represent: w the width of a digit and s the space between two digits.

The analytical expression for C_p^{int} is given by [8]:

$$C_p^{\text{int}}[F]=\varepsilon_0\varepsilon_r\frac{[nw+(n-1)s]l}{t}, \quad (8)$$

where: $\varepsilon_0=\frac{1}{36\pi\cdot10^9}\,\text{F/m}$, ε_r is the relative permittivity of the substrate, n is the number of digits, l is the length of the interdigital capacitor, w is the width of one digit, s is the space between two digits and t is the thickness of the dielectric.

Finally, the value for L_p^{stub} can be computed using relation [8]:

$$L_p^{\text{stub}}[H]=\frac{Z_C}{2\pi\cdot f}\cdot\tan\frac{2\pi\sqrt{\varepsilon_r}\cdot f\cdot l_{stub}}{c_0}, \quad (9)$$

where: f is the working frequency, Z_c is the characteristic impedance of the shunt stub inductor, l_{stub} is the length of the transmission line and c_0 is the velocity of light in vacuum.

In order to compute C_p^{stub} we use relation (8) considering only one digit.

The next step is to group the lumped elements by their effect, emphasizing the Right Handed behavior denoted by the index "R" and Left Handed behavior of the structure, denoted by the index "L" [1]:

$$\begin{aligned} L_R &= L_S^{\text{int}} \\ C_R &= 2C_p^{\text{int}}+C_p^{\text{stub}} \\ L_L &= L_p^{\text{stub}} \\ C_L &= C_S^{\text{int}} \end{aligned} \quad (10)$$

The dielectric used for implementation is a 1.524 mm thick one with 3.02 dielectric constant, 0.0013 dielectric loss tangent and Cooper metallization with 35μm thickness.

Taking into account the technological limitations, the width of the digits and distance between them is set to 0.1mm, the number of digits is n=6 and the length of one digit is *l*=5mm.

After computing the values of the lumped elements for the equivalent circuit using relations (1)-(8), we obtain:

$$L_S^{\text{int}}=2.77\text{nH},\ C_S^{\text{int}}=0.25\text{pF},\ C_p^{\text{int}}=0.09\text{pF},$$
$$C_p^{\text{stub}}=0.06\text{pF}.$$

We need to set the length and width of the shunt stub inductor. In order to do this, we set the central frequency to f_0=4.5GHz and take into account that [5]:

$$f_0=\frac{1}{2\pi\sqrt[4]{L_L C_L L_R C_R}} \quad (11)$$

After some manipulations, we set the length of the stub to 5.75 mm and the width to 0.65 mm.

The number of cells used to create the final structure is three and the symmetry of the cell is a "T" one, as Fig. 3 shows. Also, another aspect considered and shown in Fig. 3 is the fact that the access ports have 50 Ω, while the corresponding impedance given by the width of the interdigital capacitor is different, around 107 Ω.

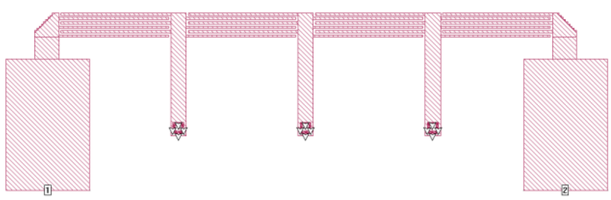

Fig. 3. Metamaterial main structure with three unit cells in microstrip technology

The simulation is run using Sonnet Software and the results are given in Fig. 4 [9].

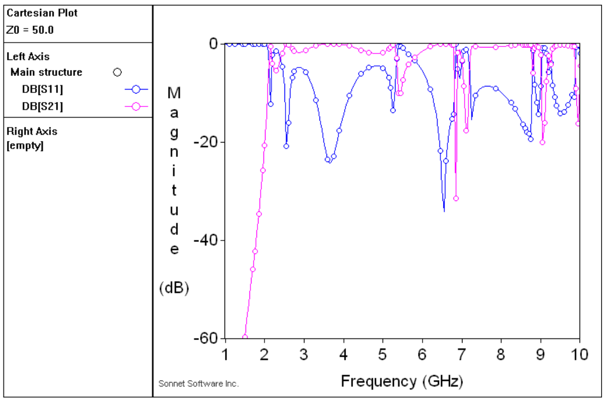

Fig. 4. Electromagnetic simulation results for the main structure

Analyzing Fig. 4, we observe that the structure is slightly unbalanced and also, because of the relative small number of unit cells used to create the metamaterial, some ripples appear in the pass-band. Box resonances estimated by the software based on lossless empty cavity are: 5.346 GHz - TE Mode 1,0,1, respectively 6.827 GHz - TE Mode 2,0,1 and they can be observed on the graph as well.

We can identify the bandwidths where the metamaterial acts as a Left Handed structure from 2.25GHz to 4.5GHz, respectively as a Right Handed one from 4.5GHz to 8.75GHz.

In literature, it is demonstrated that in order to obtain a diplexer, different types of metamaterials are needed [1], [10], because the strong coupling phenomenon is achieved when one metamaterial acts as a LH medium, while the other one acts as a RH medium and vice versa. Also, the level of coupling is given by the number of unit cells that is used and the distance between the coupled structures [1].

So, we want to design a diplexer with 3dB coupling attenuation and using the same type of metamaterial as the main structure. In order to do this, we create the second metamaterial which consists of unit cells two times smaller than the main ones, assuring a frequency shift of the propagation phenomenon and the LH behavior [6]. Accordingly to relation (1) if l and l_{stub} are half the initial value, then so are the values for L_R, C_R, C_L and L_L. In this case the properties of the second type of metamaterial are shifted to frequencies two times higher, as Fig. 5 shows [9].

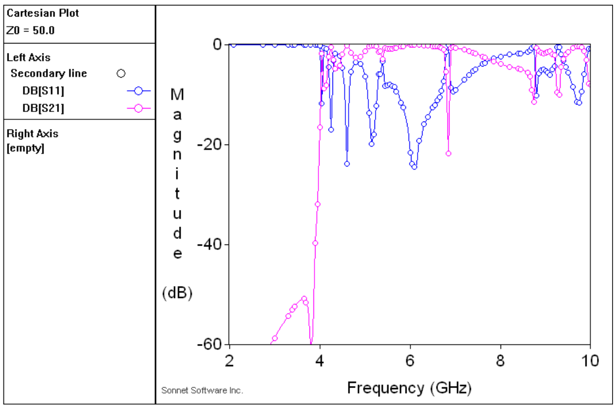

Fig. 5. Electromagnetic simulation results for the secondary structure

Analyzing Fig. 5, one can observe the frequency shift, meaning that the secondary structure acts as a LH medium from 4GHz to 8.25GHz and as a RH medium from 8.25GHz to 10GHz.

Also, there are can be noticed the box resonances at: 5.347 GHz - TE Mode 1,0,1; 6.827 GHz - TE Mode 2,0,1; 9.168 GHz - TM Mode 1,1,0; 9.791 GHz - TE Mode 1,0,2. The box resonances do not affect the coupling phenomenon that we are interested in as measurement results show.

3. Results

In order to obtain the 3dB diplexer, we couple the two metamaterials at a distance of 0.1mm. This distance assures a high level of coupling, even if the number of cells is reduced. The structure is implemented in microstrip technology as shown in Fig. 6. The overall dimensions are 3X2cm.

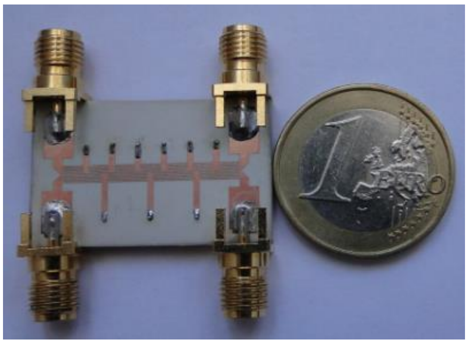

Fig. 6. Miniaturized metamaterial diplexer

A microscopic image of the unit cells is given in Fig. 7, showing the importance of the technological precision of such structures as the theoretical analysis imposes.

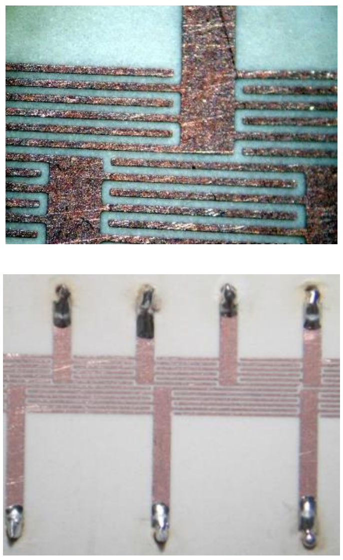

Fig. 7. Microscopic view of the metamaterial coupled structures

The measurements for this diplexer are made in the frequency bandwidth 100kHz-8,5GHz with the vectorial network analyzer Agilent E5072. In all measurements Port 1 is considered the input port of the diplexer.

We then identify ports 2 and 3 output ports and port 4, isolated one.

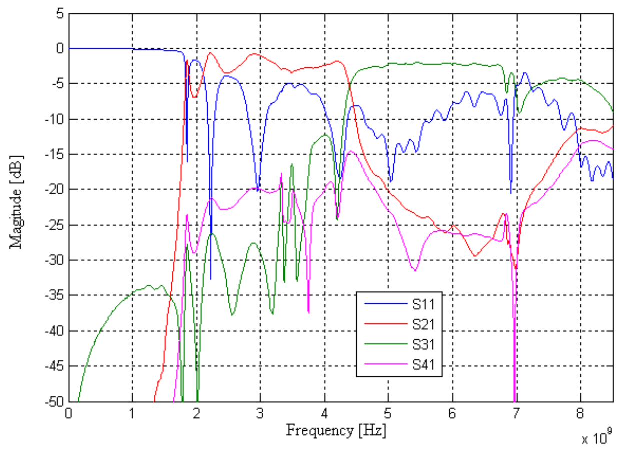

Fig. 8. Measured parameters of the proposed diplexer

Fig. 8 shows the frequency behavior of the diplexer. It is clear that the transfer of power from the input port is done on the main structure from 2GHz to 4.25GHz, while from 4.25GHz to 7GHz the transfer of power is done on the secondary structure. The transfer of power on the secondary line corresponds mainly to the domain of frequencies where the main line has a RH behavior and the secondary line has a LH behavior. This proves that the theory presented earlier is correct.

Next we analyze the simulated parameters and the measured ones to better understand the differences. In Fig. 9, there are given the transfer parameters obtained after simulation and measurement.

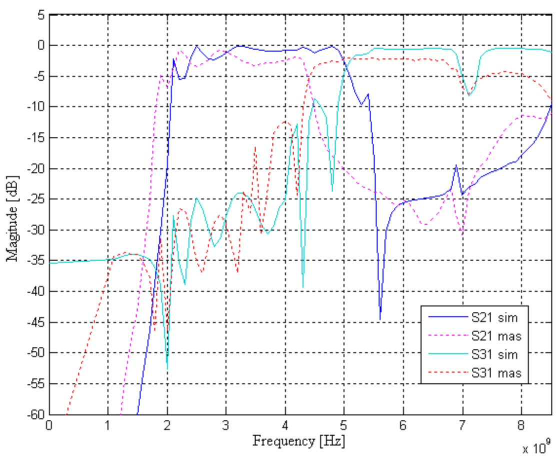

Fig. 9. Simulated and measured transfer parameters

Analyzing Fig. 9, we notice that there are differences between the simulated and measured results. First, there is a frequency shift to lower frequencies in the measured case and the level of transferred power is around 3dB rather than 0.5dB as in the simulated case. Still, we have the behavior of a diplexer with two channels.

In Fig. 10, there are given the results for return loss after simulation and measurement. It can be seen that in the interest bandwidth, from 2GHz to 7GHz, the results are satisfactory.

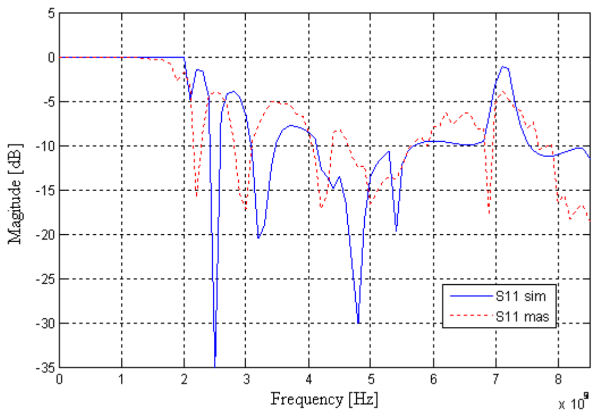

Fig. 10. Simulated and measured return loss

Last but not least, the results obtained after measurement for the isolation loss are better than the simulated ones, as Fig. 11 shows. In the working bandwidth of the diplexer, the measured isolation loss is less than 20dB.

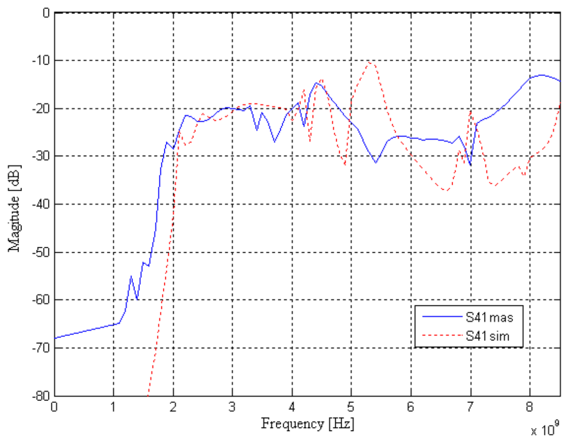

Fig. 11. Simulated and measured isolation loss

The results obtained after measurement show thatit can be used with microwave receivers or transmitters on different, widely separated, frequency bands. It can also be used for a multi-band antenna, with a common feedline. The frequncy bands of both channels are very wide.

4. Conclusions

In this paper a novel minimized diplexer is proposed, optimized, simulated and implemented in microstrip technology. First, an analytical model and computational relations are introduced as a starting point in the design of the structure. Then, full-wave electromagnetic analysis is carried to confirm the propagation phenomenon expected to appear on the proposed metamaterial structures. The number of unit cells are reduced in order to minimize as much as possible the device, but to keep the desired performances imposed by design.

The two structures are coupled at a distance of 0.1mm in order to achieve a 3dB coupling which is unavailable with conventional coupled materials.

The novel device confirms the coupling phenomenon which appears on two different types of metamaterials: the power propagating on the main structure acting as a RH medium is fully transferred on the secondary structure acting as a LH medium. This phenomenon can not be found in the case of conventional materials.

The dielectric used for implementation is a 1.524 mm thick one with 3.02 dielectric constant, 0.0013 dielectric loss tangent and Cooper metallization with 35μm thickness and the dimensions of the whole structure is 2X3cm.

The measurements show that the diplexer can be used for a relatively large bandwidth from 2GHz to 4.25GHz, respectively from 4.25GHz to 7GHz with good performances.

Acknowledgment

The work has been funded by the Sectoral Operational Programme Human Resources Development 2007-2013 of the Ministry of European Funds through the Financial Agreement POSDRU/159/1.5/S/134398.

This work was supported in part by a grant of the Romanian National Authority for Scientific Research, Program for research - Space Technology and Advanced Research - STAR, project ADANSPACE, number 63/29.11.2013".

References

[1] C. Caloz, T. Itoh, John Wiley & Sons, Inc., Hoboken, New Jersey.
[2] Colin Daniel Decle, Hu Zhirun, Microwave Conference (APMC), 2014 Asia-Pacific **213**(4-7), 211 (2014).
[3] Shih-Chia Chiu, Chien-Pai Lai, Shih-Yuan Chen, Antennas and Propagation, IEEE Transactions on **61**(3), 1071 (2013).
[4] J. H. Choi, C.-T. M. Wu, Lee Hanseung, T. Itoh, European Microwave Conference (EuMC), 2014 44th **318**(6-9) 315 (2014).
[5] A. Sanada, C. Caloz, T. Itoh, IEEE Microwave and Wireless Components Letter **14**(2), (2004).
[6] I. A. Mocanu, M. G. Banciu, N. Militaru, G. Lojewski, T. Petrescu, Proceedings 8th International Conference on Communications, 2010, Bucharest, **1**, ISBN 978-1-4244-6361-9, pp. 267-271, IEEE Catalog Number CFP1041J-ART.
[7] M. A. Buenno, A. K. T. Assis, Journal of Physics, Appl. Phys. D **28**, 1802 (1995).
[8] R. Garg, I. J. Bahl, Artech House, Dedham, 1979.
[9] *** Sonnet Software Inc., New-York – Sonnet Professional release 10.52.
[10] C. Caloz, H. V. Nguyen, Appl. Phys. A **87**, 309 (2007).

*Corresponding author: mihai.iulia83@yahoo.com